

# The $\text{Cr}_3\text{C}_2$ thermal spray coating on Al-Si substrate

M. Richert <sup>a,\*</sup>, M. Książek <sup>b</sup>, B. Leszczyńska-Madej <sup>a</sup>,  
I. Nejman <sup>a</sup>, R. Grzelka <sup>c</sup>, P. Pałka <sup>a</sup>

<sup>a</sup> Faculty of Non-Ferrous Metals, AGH University of Science and Technology,  
Al. Mickiewicza 30, 30-059 Kraków, Poland

<sup>b</sup> Foundry Institute, ul. Zakopiańska 73, 30-418 Kraków, Poland

<sup>c</sup> Plasma System S.A., ul. Wyzwolenia 3, 41-103 Siemianowice Śląskie, Poland

\* Corresponding author: E-mail address: mrichert@agh.edu.pl

Received 17.11.2009; published in revised form 01.01.2010

## Manufacturing and processing

### ABSTRACT

**Purpose:** The objective of this work was to present the changes between the plasma sprayed and high velocity oxy-fuel (HVOF) wear  $\text{Cr}_3\text{C}_2$  resistant coats. The differences in microstructure and microhardness of coatings were investigated. The characterization of fully melted, un- melted and partly melted areas was performed.

**Design/methodology/approach:** The investigated coats contained very differentiate areas, especially plasma sprayed layers. Systematic investigations of microstructure by using optical, electron scanning microscopy and transmission electron microscopy selected fully melted, un- melted or partly melted areas and their characteristic features were performed. Microhardness of coats was measured and compared with the similar literature results.

**Findings:** Microstructure of plasma sprayed coats was finding as consisting from elongating splats, additionally contained un-melted previous particle of powder and some voids and oxides. Contrary to this the HFOV coatings were more uniform containing almost equiaxial grains. The microhardness of HFOV coatings was almost two times higher than plasma sprayed ones.

**Practical implications:** The performed investigations provide information, which could be useful in the industrial practice about the essential features of wear resistant plasma sprayed coatings.

**Originality/value:** It was assumed that HVOF coatings have more uniform microstructure, higher microhardness, which could suggests better resistance before the wear and grindability.

**Keywords:** Plasma sprayed and high velocity oxy-fuel techniques; Wear resistant coatings;  $\text{Cr}_3\text{C}_2$  carbides

#### Reference to this paper should be given in the following way:

M. Richert, M. Książek, B. Leszczyńska-Madej, I. Nejman, R. Grzelka, P. Pałka, The  $\text{Cr}_3\text{C}_2$  thermal spray coating on Al-Si substrate, Journal of Achievements in Materials and Manufacturing Engineering 38/1 (2010) 95-102.

## 1. Introduction

The different coating technologies nowadays are more often applied to surface covering of intermediate products and industrial goods [1, 2]. The wear resistant coatings can be also form by the physical vapour deposition technologies (PVD) [3-6]. Layers

from titanium aluminium nitride, chromium carbides can be easily deposited on different substrates. This method is especially used for tools coating. The main limitation of PVD is the size of a vacuum chamber, which restricted the size of coating elements. Therefore in some cases the plasma sprayed techniques are more convenient.

Thermal spray is a well established process for deposition and coatings for corrosion, wear protection, and thermal barrier coatings. The HVOF process is the preferred technique for spraying wear and/or corrosion resistant carbides as well as Hastelloy, Triaballo and Inconel alloys. The coatings have very high bond strengths, fine as-sprayed surface finishes and low oxide levels [1]. The authors of the work [7] found that inside coats the  $\text{Cr}_7\text{C}_3$  carbides were present around blocks of  $\text{Cr}_3\text{C}_2$  carbides. They suggest that  $\text{Cr}_7\text{C}_3$  carbides form due to the decarburization of  $\text{Cr}_3\text{C}_2$  carbides during the spraying process. Besides this type of carbides they found also small nanometric  $\text{Cr}_{27}\text{C}_6$  carbides inside NiCr matrix and stated that they precipitate during the HVOF deposition by the same mechanism as  $\text{Cr}_7\text{C}_3$  carbides. The results suggest essential influence of deposition parameters on the coatings microstructure. Therefore the final phase consistence of coatings could be different to the initial composition of depositing materials. It could change the coatings parameters and properties.

Opposite of HVOF, plasma sprayed coatings showed larger porosity, existence of more not melted droplets and oxides. Especially plasma sprayed coatings exhibit larger grains in comparison to the HVOF method and also the larger porosity substantially influenced on the hardness of plasma sprayed coatings and resistance of wear protections.

Plasma spraying and HVOF method have been successfully used to produce different kinds of coatings on the alumina substrates [8].

Feature of coatings change as nanocrystalline grains appear inside the coatings [9]. The results of the work [10] show higher friction coefficient of about 20-30% and higher hardness of about 20% for nanocrystalline coatings in comparison to  $\text{Cr}_3\text{C}_2$  (25Ni20Cr) coatings with the conventional size of grains. The obtained results suggest that refinement of coatings microstructure favour higher resistance against wear. The nanometric coatings contained less porosity but more oxidation, which are connected with the larger amount of grain boundaries. Larger amount of high energy grain boundary area of nano-powders tend to melt more easily and it causes a decreasing roughness of coating surface. The nanometric HVOF coatings show large grain refinement, in comparison to other thermal sprayed techniques, which result in better properties against wear degradation.

The interesting is hardness measurement of different thermal sprayed coatings, which results indirectly indicated resistance to wear degradation.

Sidhu et al. [10] show that microhardness of  $\text{Cr}_3\text{C}_2$  coatings was about 850 HV. The result agrees with the Scriveri et al. [11], Mann and Arya [12] and others reports. On the other hand Matthews et al. [13] found microhardness of  $\text{Cr}_3\text{C}_2$  - NiCr coatings equal 1036  $\text{HVN}_{300}$  and 1163  $\text{HVN}_{300}$  deposited respectively by HVOF and HVOF techniques. In the study [14] the hardness of  $\text{Cr}_3\text{C}_2$  - NiCr coatings, deposited by VPS (Vacuum plasma spraying) had value of 540  $\text{HV}_{300}$ .

The aim of the present study is the comparison of plasma and high velocity oxy-fuel sprayed  $\text{Cr}_3\text{C}_2$  - NiCr wear resistant coatings.

The special attention was put on the difference finding in structure and properties of coatings.

## 2. Experimental basis

The High-Velocity Oxy-Fuel spraying (HVOF) and plasma sprayed technique were used for  $\text{Cr}_3\text{C}_2$  coatings spraying.

The first industrial use of high velocity oxy fuel spraying (HVOF) took place in the beginning of 1980. Powder particles injected into the flame of HVOF guns are accelerated to much higher velocity than in the conventional spraying processes, to 650 m/s in average in the modern equipments. Therefore heat transfer is moderate and particle temperatures are relatively low. Plasma spraying is generally regarded as the most versatile of all thermal processes. An electric arc dissociates and ionizes gases as argon and hydrogen. Beyond the nozzle, the atomic components recombine giving off a tremendous amount of heat; of about 10000°C. Powder is injected into the flame, melted and accelerated on the work pieces. The successive layers of droplets are covered substrate forming coating microstructure. During the deposition process the different phenomenon appears as remelting earlier forming layers, fast diffusion or atomizing deposited materials.

The  $\text{Cr}_3\text{C}_2$  coatings with the intermediate layers of NiAl were sprayed by using high velocity oxy-fuel method (Plasma System S.A., Siemianowice Śląskie) using HP/JP 5000 Gun Kit, with oxygen 940 and kerozyna 23 l/h, melt powder particle and spray them onto the AlSi substrate. The powder selected was a commercial 80%  $\text{Cr}_3\text{C}_2$  - 20% NiCr (wt%) with the initial size of average 250  $\mu\text{m}$  and 800 nm. The spraying distance of 370 mm and gun speed 35 m/min were used.

The plasma sprayed 80%  $\text{Cr}_3\text{C}_2$  - 20% NiCr (wt%) coatings were prepared by MIM40 device. The argon 2500 l/h and hydrogen 873 l/min were used for melting powders particles before their impact onto the substrate. The spraying distance of 9.5 mm and gun speed 25 m/min were used.

The microstructure of all coatings was studied by Olympus GX50 optical and TESLA BS500 electron scanning microscopy. Thin foils were observed by JEOL 2010 ARB transmission electron microscopy with the Energy Disperse Spectrometer (EDS) for identification of chemical composition in microareas of coatings. The microhardness of coatings was measured by using PMT3 microhardness tester at load 200 G.

The samples to light microscopy observations were polished mechanically applied Struers equipment and technique. They were grinded, than polished in diamond pastes and in the suspension OPS.

Thin foils, for TEM investigations, were prepared from cross sections by cutting grinding and ion sputtering, using Struers and Gatan instruments.

The investigations of phase composition of plasma sprayed and HVOF coatings were performed by using Bruker D8 Discover-Advance diffractometer with copper lamp (40 kV, 30 mA,  $\lambda=1.540598$  Å). The method measurement superficial layer and software Diffract Plus Evaluation was used for inspect of layers composition.

## 3. Investigation results

The microstructure of  $\text{Cr}_3\text{C}_2$ -NiCr coatings prepared by plasma sprayed technique is non-homogeneous (Fig. 1). The fully melted volumes form elongating splats. However between them

the equiaxial grains are visible, which probably are the un-melted powder particles.

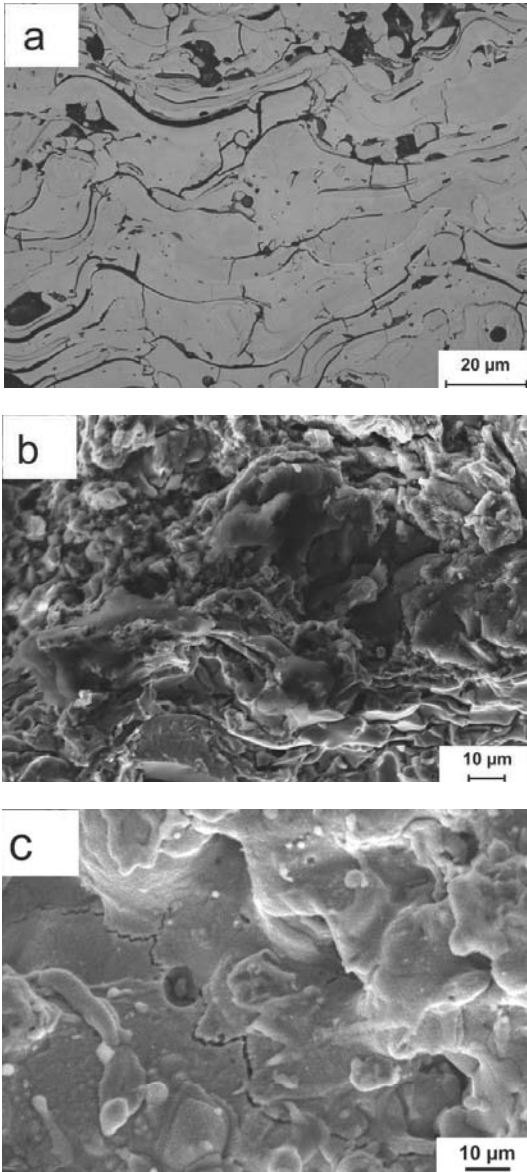


Fig. 1. Characteristics microstructure of plasma sprayed  $\text{Cr}_3\text{C}_2\text{-NiCr}$  coating

The scanning electron micrographs show general aspect of the as-deposits microstructure. Some particles did not fully melt into the flame retained in the coatings (Fig. 1b). It confirms the observations performed by using light microscope techniques. The 3D view, observed by SEM, exhibits the details of plasma sprayed coatings. Inside elongating splats the internal boundaries were found dividing splats into small domains.

Pores and oxides appeared as black places inside the coatings (Figs. 1a, 1b). Pores and oxides mainly are placed at grain boundaries, which is unprofitable feature of plasma sprayed coatings.

It could be also found some cracks of coatings, during the observations performed at higher magnifications by using SEM techniques. They probably are connected with the stacking of oxides and pores or as a result of tensile residual stresses (Fig. 1c). The tensile residual stresses inside the coatings appeared due to large differences between the temperature of deposited materials and the temperature of substrate. The second reason of cracks could be connected with the fast cooling of coating materials which can also contribute to the arise of residuals stresses. Next the differences in value of coefficient of expansion can also influence on the appearing of cracks.

The microhardness of  $\text{Cr}_3\text{C}_2\text{-NiCr}$  coatings was measured to be around  $330 \mu\text{HV}$ , the intermediate layer NiAl  $300 \mu\text{HV}$  and AlSi substrate  $72 \mu\text{HV}$ . The profile of microhardness through thickness is presented at Fig. 2. The microhardness of substrate is about 80% lower than microhardness of the outer coating.

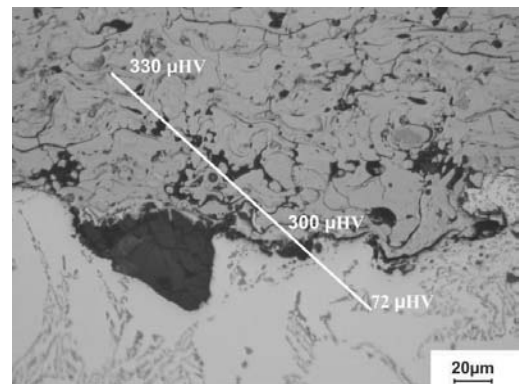


Fig. 2. Structure of plasma sprayed coating with the microhardnes levels

In comparison to the literature data, the measured hardness of  $\text{Cr}_3\text{C}_2\text{-NiCr}$  outer coating is lower of about 30% than microhardness of  $\text{Cr}_3\text{C}_2\text{-NiCr}$  coating prepared by Vacuum Plasma Spraying, investigated by Marcano et al. [14]. It suggests that investigated coatings are probably much more porous than Marcano samples and additionally the cracks found inside the coatings can contribute to the microhardness reduction.

The plasma spraying  $\text{Cr}_3\text{C}_2\text{-NiCr}$  coatings show differentiate thickness from  $220 \mu\text{m}$  to  $360 \mu\text{m}$ , as it is visible at Fig. 3. They show very good adherence to the substrate and fulfilling all roughness of surface.

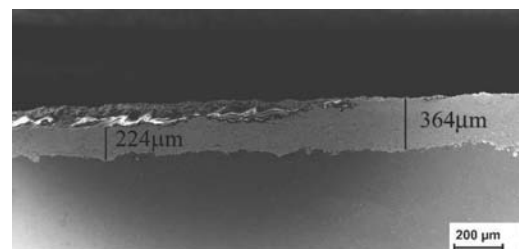


Fig. 3. Plasma sprayed coating on the AlSi substrate

The average  $200\text{-}300 \mu\text{m}$  thickness of plasma sprayed coatings was found by measurement using light microscope

techniques. In comparison to the literature data, the thickness of the investigated coatings is placed inside the range of usually obtained thickness of coatings by thermal sprayed techniques.

In majority all performed observations of interface between the substrate and coatings do not showed any cracks and no gaps. It is characteristic for good connection.

Some oxides we observed as it could be visible at Fig. 2, however at observations performed at larger magnifications by using SEM technique they were not found. It proofs that the connection between the substrate and coatings exhibit not only adhesion joints but also some part of diffusion contacts.

The coatings consist from outer and intermediate layer as it is visible at Fig. 4. The deposition of intermediate layer contributes to the better connection of coatings to the substrate.

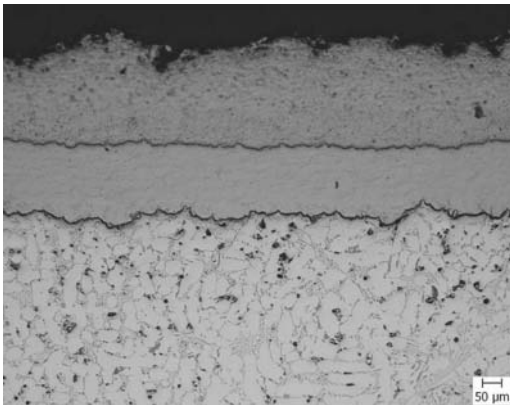


Fig. 4. Plasma sprayed coating consisting from outer and intermediate zones

In comparison to plasma sprayed coatings the microstructure of HVOF layers is more uniform (Fig. 5). The fairly equiaxial microstructure domains and very fine grain size is the characteristic feature of HVOF coatings microstructure. The microstructure observed by optical (Fig. 5a) and scanning electron microscopy (Fig. 5b) proofs that HVOF is less porous than plasma sprayed coatings. Any cracks and pores were found in the microstructure of HVOF.

The microhardness value of  $\text{Cr}_3\text{C}_2$ -NiCr HVOF coatings were found of about  $920 \mu\text{HV}_{200}$  in average (Fig. 5). It could be comparable to Matthews et al. [14], which found microhardness of  $\text{Cr}_3\text{C}_2$  - NiCr coatings equal  $1036 \text{ HVN}_{300}$  and  $1163 \text{ HVN}_{300}$  deposited respectively by HVOF and HVOF techniques.

Some differences in microhardness are probably connected with variations of spray parameters; however they could be also connected with the difference in the initial size of the splash powders. The porosity of as-splated coatings strongly can influence of the microhardness level. The profile of microhardness through HVOF coating is presented at Fig. 6.

The transmission electron micrographs show general aspects of as-deposited microstructure. The un-melted and fully melted areas were examined in the TEM. Fig.7a shows the example of the un-melted powder particle (indicated by arrow).

The microstructure retained inside un-melted particle exhibits numerous small grains, about 50 nm to 100 nm in size, which are trapped within the deformed matrix (Figs.7b, 7c).

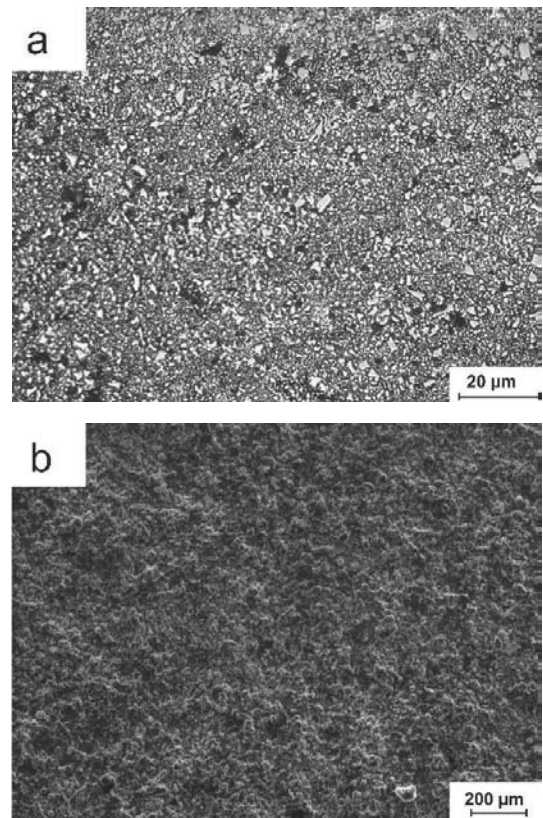


Fig. 5. Cross sectional image of HVOF,  $\text{Cr}_3\text{C}_2$ -NiCr layer

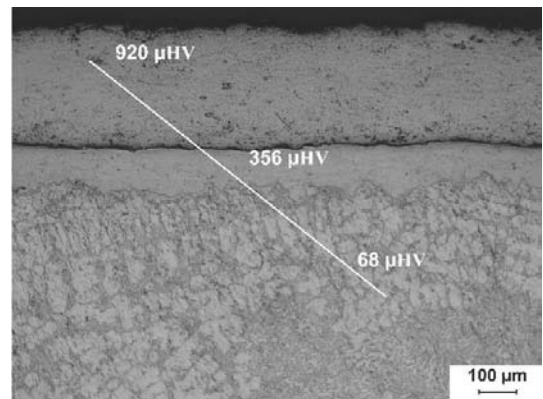


Fig. 6. Profile of microhardness through HVOF coating

The Moirés fingers observed in microstructure of HVOF coatings indicate that the observed areas are heavily deformed (Fig. 8). This is result of features of HVOF deposition. During the HVOF thermal spraying process large velocity of the deposited droplets can easily deformed earlier forming layers, also such phenomena can appear as remelting, fast diffusion or atomization of the deposited materials.

The size of small microstructure domains observed by TEM techniques was still average about 100 nm. They have equiaxial geometry.

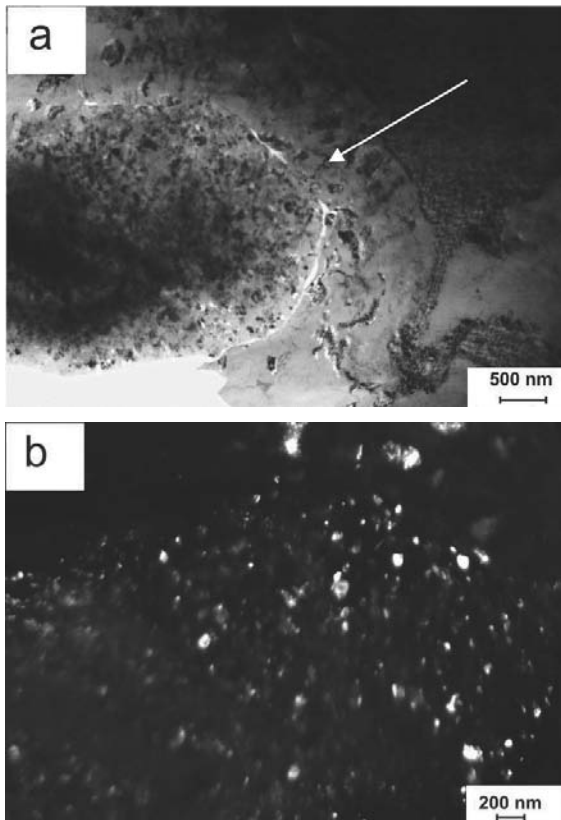


Fig. 7. Unmelted area in HVOF coating, a) micrometric particle of initial powder, indicated by arrow b) numerous small grains inside un-melted particle (dark field)

Fig. 9 shows the example of the columnar grain microstructure, which was the main feature observed inside the fully melted splats. In the performed investigations columns have about 200-300 nm in thickness, but several hundred lengths. Similar structural effects were observed by J.Gang et al. [15].

The just melted columns show characteristic spreading of deposited material (Fig. 9a). During the deposition progress the earlier melted areas are deformed and some density of dislocations appeared inside the columns (Fig. 9b).

The investigations show the flowability in connection of un-melted and fully melted regions of coatings. The un-melted areas contain nanometric in size (40-50 nm), numerous grains and they are placed adjacent the fully melted column microstructure. The fully melted areas contained very characteristic dense dislocation forests placed inside or neighbouring to columns (Fig. 9). Such microstructure proofs that during the process of deposition the hardening of depositing layers took place, which contributes to the increase of coating hardness.

The chemical composition of nanometric grains from un-melted regions was investigated by EDS technique. They contained Ni, Cr and C elements (Fig. 10). Contrary to this region inside fully melted areas Ni chemical element was dominated.

Characteristic feature of particles and nanograins observed inside the un-melted or partly melted areas or inside initial powder particles is their collection in larger clusters, which

example is visible at Fig. 10. The characteristic contrast appears at observed cluster of particles. The clusters of carbides are rich in such elements as Cr, C, and Fe. The nickel element is connected with the matrix signal surrounding the carbide particles.

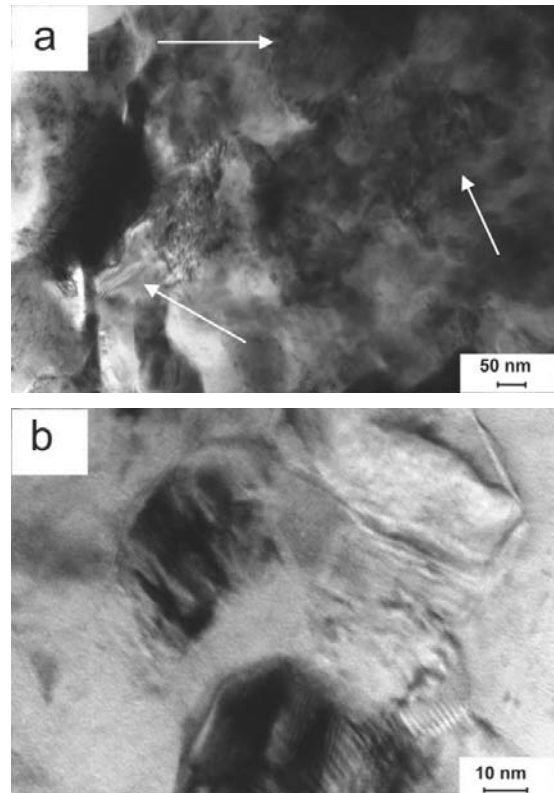


Fig. 8. Microstructure of HVOF coatings a) Moiré fingers in heavily deformed areas indicated by arrows, b) characteristic nanograins with the equiaxial shape

The agglomeration or precipitation of the carbides, which could change its chemical initial composition is not profitable and could cause reduction of the film hardness, therefore it, would be of interest to characterize the chemical form of carbides occurring inside thermal sprayed coatings.

The detailed investigation of phase composition of HVOF and plasma sprayed coatings were performed by X-ray technique. The results are presented at Fig. 11 and Fig. 12.

The suitable for wear resistant coatings,  $\text{Cr}_3\text{C}_2$  carbides were found inside the HVOF coatings (Fig. 11). Contrary to this result inside the plasma sprayed investigated volumes of coatings  $\text{Cr}_3\text{C}_2$  carbides were not found (Fig. 12).

The HVOF samples besides  $\text{Cr}_3\text{C}_2$  carbides contained also other kind of carbides such as  $\text{Cr}_7\text{C}_3$  and  $\text{Cr}_{23}\text{C}_6$ , which were found in significant quantity.

In plasma sprayed coatings  $\text{Cr}_7\text{C}_3$  carbides were dominating, however  $\text{Cr}_{23}\text{C}_6$  carbides were also identified.

The results indicate that the thermal sprayed processes can change the initial composition of the phase consistence of deposited powder, which primarily contained  $\text{Cr}_3\text{C}_2$  carbides encircled by Ni.

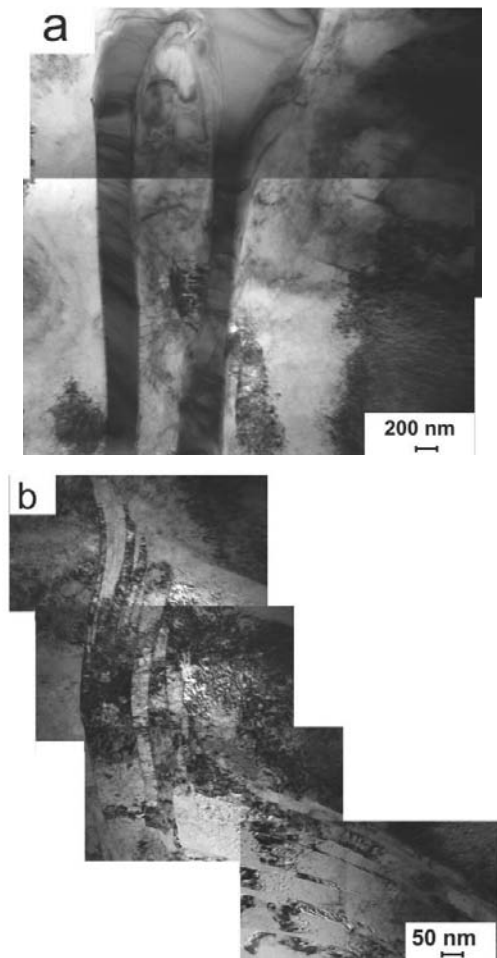


Fig. 9. Column microstructure inside fully melted regions

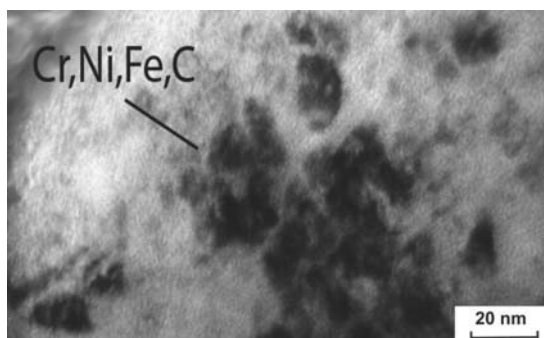


Fig. 10. Nanograins and nanoparticles in un-melted region

Especially the essential changes of phase composition were found inside the plasma sprayed coatings.

The  $\text{Cr}_7\text{C}_3$  and  $\text{Cr}_{23}\text{C}_6$  might present according to the reported results through X-ray diffraction analyses [7]. It is likely that these carbides are formed through decarburization of  $\text{Cr}_3\text{C}_2$ . However the presence of  $\text{Cr}_7\text{C}_3$  and  $\text{Cr}_{23}\text{C}_6$  in the as-sprayed coating cannot be proven solely by X-ray diffraction approach

because their main diffraction peaks partly coincide with the lines referring to the NiCr and  $\text{Cr}_3\text{C}_2$ .

Moreover, as HVOF cermets coating is usually deposited in an ambient condition, the decarburization of  $\text{Cr}_3\text{C}_2$  seemed to be associated with oxidation of  $\text{Cr}_3\text{C}_2$  and heating of spray particles [7].

The observed differences in carbides composition in HVOF and plasma sprayed coatings depend both on parameters of deposition and conditions of solidification of deposited droplets on the substrate, which strongly influence on the coating microstructure [18].

#### 4. Discussion of results

The very useful technology for production of nanometric coatings is high velocity oxygen fuel thermal spray process (HVOF) [1, 8, 10]. Obtained in the present work results indicate that the HVOF coatings are denser than plasma sprayed ones, about which proofs microhardness measurements. The microhardness of HVOF was about 60% higher than the plasma sprayed coatings.

Such result indicates that HVOF coatings should be less abrasive and have higher wear resistance than plasma sprayed ones. However such conditions as smoothness, thickness and residual compressive stresses also strongly influenced on the coatings properties.

It was noticed that the increase of HVOF layer microhardness results generally from the refinement of microstructure and decreasing its porosity. The mechanisms of HVOF microstructure diminishing depends on parameters of HVOF technology and features of the initial powder suspension [16]. Results of Jianhong and Schoenung work [17] showed the importance of the influence of feedstock powders on the microstructure coatings. Also results of Formanek et al. [18] confirm the importance of the features feedstock.

The complex form of thermal sprayed coatings, which form multilayer stacks results from necessity of good cohesion between the coatings and substrate. The intermediate layer makes possible deposition of optionally outer layer even its features are not preserve good contact with substrate.

In HVOF  $\text{Cr}_3\text{C}_2$ -NiCr coating, apart from  $\text{Cr}_3\text{C}_2$  carbide particles, the carbides  $\text{Cr}_7\text{C}_3$  and  $\text{Cr}_{23}\text{C}_6$  were presented according to the results through X-ray diffraction. The work of Ji et al [7] pointed out that the rebounding-off of the  $\text{Cr}_3\text{C}_2$  particles during coating formation is mainly responsible for the carbon loss and the change of carbide content. Such phenomenon was found in plasma sprayed coatings, in which  $\text{Cr}_3\text{C}_2$  particles were reduced after the spraying and only  $\text{Cr}_7\text{C}_3$  and  $\text{Cr}_{23}\text{C}_6$  were dispersed in NiCr alloy matrix with a nano-crystalline microstructure.

The results of work [19] report that carbides form slowly below  $300^\circ\text{C}$  and rapidly between  $300$  and  $600^\circ\text{C}$ . This correlates with the hardness behaviour between  $20$  and  $600^\circ\text{C}$ . X-ray diffraction data indicate the formation of a  $\text{Cr}_7\text{C}_3$  bulk phase above  $600^\circ\text{C}$  and  $\text{Cr}_{23}\text{C}_6$  a bulk phase above  $700^\circ\text{C}$ . This agglomeration or precipitation of the carbides results in reduction of the film hardness. It correlates with the found essentials reduction of plasma sprayed coatings in comparison to HVOF.

From this point of view, the HVOF method could be recommended for coating in the strong unfavourable wear working conditions.

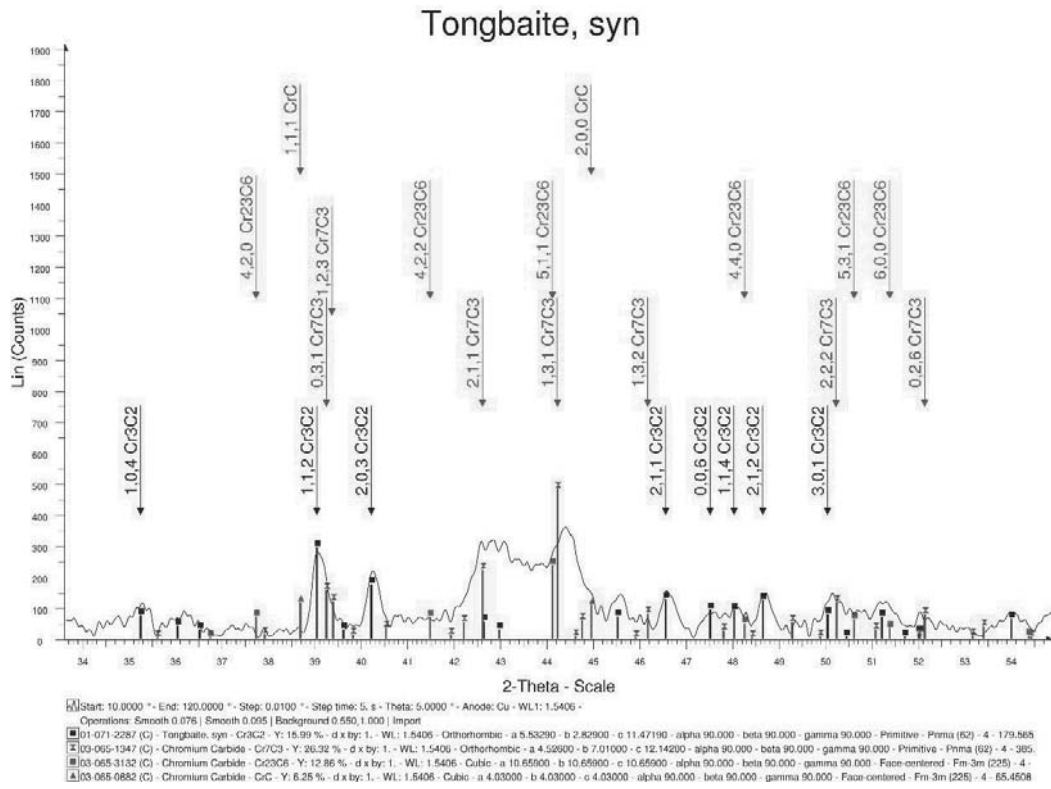


Fig. 11. Phase composition of HVOF coatings

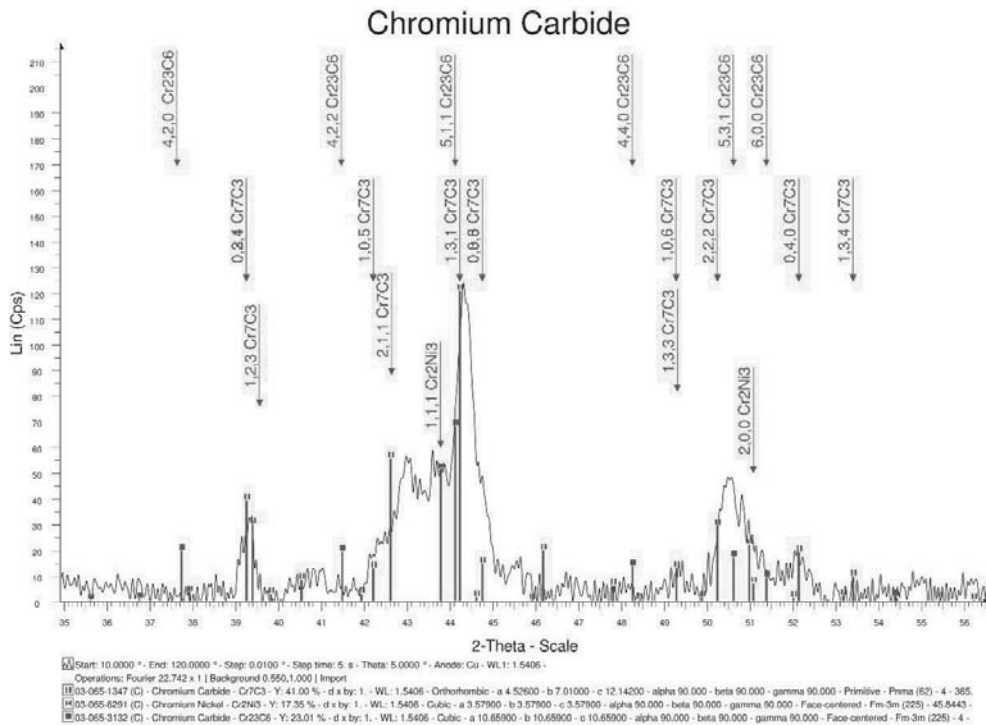


Fig. 12. Phase composition of plasma sprayed coatings

## 5. Conclusions

1. The high velocity oxy-fuel sprayed coatings show more uniform and fine grained microstructure than plasma sprayed.
2. Microhardness of HVOF coatings was about 60% higher than plasma sprayed.
3. Inside the un-melted or partly melted areas nano-grains were found. Inside fully melted areas columns with 200-300 nm in thickness and long of about several hundred nanometres were observed.
4. X-ray investigations show decarburization of  $\text{Cr}_3\text{C}_2$  during plasma sprayed and HVOF deposition. Formation of a  $\text{Cr}_7\text{C}_3$  and  $\text{Cr}_{23}\text{C}_6$  phases results in reduction of the film hardness.

## Acknowledgements

The work was financially supported by polish project No NR15 0001 06/2009.

## References

- [1] B. Wielage, A. Wank, H. Pokhmurska, T. Grund, Ch. Rupprecht, G. Reisel, E. Friesen, Development and trends in HVOF spraying technology, *Surface and Coatings Technology* 201 (2006) 2032-2037.
- [2] C. Tendero, Ch. Tixier, P. Tristant, J. Desmaison, P. Leprince, Atmospheric pressure plasma: A review, *Spectrochimica Acta B* 61 (2006) 2-30.
- [3] K. Lukaszewicz, L.A. Dobrzański, A. Zarychta, L. Cinha, Mechanical properties of multilayer coatings deposited by PVD techniques onto the brass substrate, *Journal of Achievements in Materials and Manufacturing Engineering* 15 (2006) 47-52.
- [4] L.A. Dobrzański, K. Gołombek, J. Mięka, D. Pakuła, Multilayer and gradient PVD coatings on the sintered tool materials, *Journal of Achievements in Materials and Manufacturing Engineering* 31/2 (2008) 170-190.
- [5] D. Pakuła, L. Dobrzański, Investigation of the structure and properties of PVD and CVD coatings deposited on the  $\text{Si}_3\text{N}_4$  nitride ceramics, *Journal of Achievements in Materials and Manufacturing Engineering* 24/2 (2007) 79-82.
- [6] L.A. Dobrzański, L. Wosińska, K. Gołombek, J. Mięka, Structure of multicomponent and gradient PVD coatings deposited on sintered tool materials, *Journal of Achievements in Materials and Manufacturing Engineering* 20 (2007) 99-102.
- [7] G.-Ch. Ji, Ch.-J. Li, Y.-Y. Wang, W.-Y. Li, Microstructural characterization and abrasive wear performance of HVOF sprayed  $\text{Cr}_3\text{C}_2$  - NiCr coating, *Surface and Coatings Technology* 200 (2006) 6749-6757.
- [8] J.A. Picas, A. Forn, R. Rilla, E. Martin, HVOF thermal sprayed coatings on aluminium alloys and aluminium matrix composites, *Surface and Coatings Technology* 200 (2005) 1178-1181.
- [9] M. Roy, A. Pauschitz, R. Polak, F. Franek, Comparative evaluation of ambient temperature friction behavior of thermal sprayed  $\text{Cr}_3\text{C}_2$  - 25(Ni20Cr) coatings with conventional and nano-crystalline grains, *Tribology International* 39 (2006) 29-38.
- [10] H.S. Sidhu, B.S. Sidhu, S. Prakash, Mechanical and microstructural properties of HVOF sprayed WC-Co and  $\text{Cr}_3\text{C}_2$  - NiCr coatings on the boiler tube steel using LPG as the fuel gas, *Journal of Materials Processing Technology* 171 (2006) 77-82.
- [11] A. Scriveri, S. Ianelli, A. Rossi, R. Groppetti, F. Casadei, G. Rizzi, A contribution to the surface analysis and characterization of HVOF coatings for petrochemical application, *Wear* 250 (2001) 107-113.
- [12] B.S. Mann, V. Arya, Abrasive and erosive wear characteristics of plasma nitriding and HVOF coatings: their application in hydro turbines, *Wear* 249 (2001) 354-360.
- [13] S. Matthews, B. James, M. Hyland, The role of microstructure in the mechanism of high velocity erosion of  $\text{Cr}_3\text{C}_2$  - NiCr thermal spray coatings: Part1 - As - sprayed coatings, *Surface and Coatings Technology* 203 (2009) 1086-1093.
- [14] Z. Marcano, J. Lesage, D. Chicot, G. Mesmacque, E.S. Puchi-Cabrera, M.H. Staia, Microstructure and adhesion of  $\text{Cr}_3\text{C}_2$  - NiCr vacuum plasma sprayed coatings, *Surface and Coatings Technology* 202 (2008) 4406-4410.
- [15] J. Gang, J.-P. Morniroli, T. Grosdidier, Nanostructures in thermal spray coatings, *Scripta Materialia* 48 (2003) 1599-1604.
- [16] H. Jianhong, J.M. Schoenung, Nanostructured coatings, *Materials Science and Engineering, A* 336 (2002) 274-319.
- [17] B. Formanek, K. Szymański, A. Beliyev, Composite carbide powders and HVOF sprayed coatings with a plastic matrix, *Journal of Achievements in Materials and Manufacturing Engineering* 18 (2006) 351-354.
- [18] E.-S. Lee, W.-J. Park, K.-H. Baik, S. Ahn, Different carbide types and their effect on bend properties of a spray-formed high speed steel, *Scripta Materialia* 39/8 (1998) 1133-1138.
- [19] G.N. Salaita, G.B. Hoflund, „Dynamic SIMS study of  $\text{Cr}_3\text{C}_2$ ,  $\text{Cr}_7\text{C}_3$  and  $\text{Cr}_{23}\text{C}_6$ , *Applied Surface Science* 134 (1998) 194-196.